

Determination of constitutive and morphological parameters of columnar thin films by inverse homogenization

Tom G. Mackay¹

*School of Mathematics and Maxwell Institute for Mathematical Sciences
University of Edinburgh, Edinburgh EH9 3JZ, UK*

and

*NanoMM — Nanoengineered Metamaterials Group
Department of Engineering Science and Mechanics*

Pennsylvania State University, University Park, PA 16802–6812, USA

Akhlesh Lakhtakia²

*NanoMM — Nanoengineered Metamaterials Group
Department of Engineering Science and Mechanics*

Pennsylvania State University, University Park, PA 16802–6812, USA

Abstract

A dielectric columnar thin film (CTF), characterized macroscopically by a relative permittivity dyadic, was investigated theoretically with the assumption that, on the nanoscale, it is an assembly of parallel, identical, elongated ellipsoidal inclusions made of an isotropic dielectric material that has a different refractive index from the bulk material that was evaporated to fabricate the CTF. The inverse Bruggeman homogenization formalism was developed in order to estimate the refractive index of the deposited material, one of the two shape factors of the ellipsoidal inclusions, and the volume fraction occupied by the deposited material, from a knowledge of relative permittivity dyadic of the CTF. A modified Newton–Raphson technique was implemented to solve the inverse Bruggeman equations. Numerical studies revealed how the three nanoscale parameters of CTFs vary as functions of the vapour incidence angle.

Keywords: Bruggeman homogenization formalism, Newton–Raphson technique, tantalum oxide, titanium oxide, zirconium oxide

1 Introduction

Columnar thin films (CTFs) are familiar structures within the optics literature, having been fabricated by physical vapour deposition methods for well over a century [1]. Their morphology is reminiscent of certain crystals, while their macroscopic optical properties are analogous to those of certain orthorhombic crystals. Furthermore, they are the precursors of the more complex sculptured thin films (STFs) [2].

The prospect of controlling the porosity and the columnar morphology of these thin films at the fabrication stage, in order to engineer their macroscopic optical responses, renders them attractive platforms for optically sensing chemical and biological species [3, 4, 5, 6, 7, 8, 9, 10, 11]. However, for intelligent design and deployment of such sensors, it is important to fully characterize the relationship between macroscopic constitutive properties on the one hand and the nanoscale morphology and composition on the other.

There are significant impediments towards arriving at definitive relationships. One is the variability that exists due to differences in deposition conditions [12, 13]. For instance, the bulk material that is evaporated

¹E-mail: T.Mackay@ed.ac.uk.

²E-mail: akhlesh@psu.edu

may be quite different from the material that is actually deposited as a thin film. Therefore, while the dielectric properties of the bulk material is easily known prior to evaporation, the dielectric properties of the deposited material may well be different, depending on, whether the deposition occurred in an oxidizing or reducing atmosphere, whether trace amounts of water vapor were present, and the temperature. As an example, when Ti_2O_3 is evaporated, the deposited material has been shown by one research group to be either $\text{TiO}_{1.8}$ or $\text{TiO}_{1.5}$, depending on whether the temperature is 25°C or 250°C [14]. Evaporation of different suboxides of titanium leads to the deposition of different TiO_α films, in general, where the real number α varies with the nominal deposition conditions and even the deposition apparatus. Likewise, when SiO_2 is evaporated, the deposited material is some ill-defined but consistent mixture of Si and SiO_2 and is thus often classified as SiO_α , $\alpha \in (1, 2)$ [15, p. 164]. Furthermore, the delineation of nanoscale morphology is not an unambiguous task, as even a cursory glance at scanning-electron-microscope images of CTFs will confirm [1]. Direct determination of porosity or void volume-fraction through a gas-adsorption technique [16, 17, 18], although accurate, is very time-consuming. Therefore, porosity is usually measured indirectly through measurement of mass density, which has its own sources of inaccuracy [12].

Various researchers [1, 19, 20, 21, 22] have put forth nanoscale-to-macroscopic models for the relative permittivity dyadics of CTFs. Generally speaking, in these models the CTF is viewed as an assembly of parallel, identical, nanoscale inclusions of a certain shape dispersed in a certain homogeneous material. At optical and lower frequencies, these inclusions are electrically small and can therefore be homogenized into a macroscopically homogeneous material [23]. Apart from the shape of the inclusions, one must choose the porosity and the bulk dielectric properties of the deposited material and the material in the void regions (usually taken to be air) of the CTF. Such models require careful calibration against experiments [24].

Inversion of the *forward* homogenization procedure can provide nanoscale information about a CTF, which can be useful, for example, to predict what would happen if the CTF were to be infiltrated by some other material [25]. This thought motivated the work reported in this paper.

Provided the components of the relative permittivity dyadic of a CTF are measured by suitable optical experiments [26, 27], an *inverse* homogenization procedure could yield the refractive index of the deposited material, the porosity of the CTF, and the shape of the inclusions, if certain reasonable assumptions are made. A demonstration based on the Bruggeman formalism [28] is presented in the following sections. In the notation adopted here, vectors are underlined whereas dyadics are double underlined. The unit Cartesian vectors are written as \underline{u}_x , \underline{u}_y , and \underline{u}_z ; the unit dyadic $\underline{\underline{I}} = \underline{u}_x \underline{u}_x + \underline{u}_y \underline{u}_y + \underline{u}_z \underline{u}_z$; the permittivity of free space is denoted by ϵ_0 ; the angular frequency is denoted by ω ; and $i = \sqrt{-1}$.

2 Homogenization model

Let us consider a CTF grown on a planar substrate through the deposition of an evaporated bulk material. The planar substrate is taken to lie parallel to the $z = 0$ plane, and the deposited material is assumed to be an isotropic dielectric material with refractive index n_s . At length scales far greater than the nanoscale, the CTF is effectively a continuum which may be characterized by the frequency-domain constitutive relation [1, 2]

$$\underline{D} = \epsilon_0 \underline{\underline{\epsilon}}_{CTF} \cdot \underline{E}, \quad (1)$$

where

$$\underline{\underline{\epsilon}}_{CTF} = \underline{\underline{S}}_y(\chi) \cdot (\epsilon_a \underline{u}_z \underline{u}_z + \epsilon_b \underline{u}_x \underline{u}_x + \epsilon_c \underline{u}_y \underline{u}_y) \cdot \underline{\underline{S}}_y^{-1}(\chi) \quad (2)$$

is the relative permittivity dyadic of the CTF. The middle dyadic on the right side of Eq. (2) indicates the macroscopic orthorhombic symmetry of the CTF [1]. The orientation of the columns with respect to any xy plane is indicated via the inclination dyadic

$$\underline{\underline{S}}_y(\chi) = \underline{u}_y \underline{u}_y + (\underline{u}_x \underline{u}_x + \underline{u}_z \underline{u}_z) \cos \chi + (\underline{u}_z \underline{u}_x - \underline{u}_x \underline{u}_z) \sin \chi, \quad (3)$$

where the column inclination angle is $\chi \in (0, \pi/2]$.

Each column of the CTF may be regarded as a set of elongated ellipsoidal inclusions strung together end-to-end. All inclusions have the same orientation and shape. The latter is specified through the shape dyadic

$$\underline{\underline{U}}_s = \underline{u}_n \underline{u}_n + \gamma_\tau \underline{u}_\tau \underline{u}_\tau + \gamma_b \underline{u}_b \underline{u}_b, \quad (4)$$

wherein the normal, tangential, and binormal basis vectors are specified in terms of the column inclination angle per

$$\left. \begin{aligned} \underline{u}_n &= -\underline{u}_x \sin \chi + \underline{u}_z \cos \chi \\ \underline{u}_\tau &= \underline{u}_x \cos \chi + \underline{u}_z \sin \chi \\ \underline{u}_b &= -\underline{u}_y \end{aligned} \right\}. \quad (5)$$

Since the columnar morphology is highly aciculate, we have that the shape parameters $\gamma_b \gtrsim 1$ and $\gamma_\tau \gg 1$. As increasing γ_τ beyond 10 does not have significant effects for slender inclusions, we fixed $\gamma_\tau = 15$ for definiteness.

As the CTF is porous, we introduce $f \in (0, 1)$ as the volume fraction occupied by the ellipsoidal inclusions representing the columns of the CTF. The void region is filled with air (or vacuum). Thus, the porosity of the CTF equals $1 - f$.

3 Forward and inverse homogenization

The nanoscale parameters $\{n_s, f, \gamma_b\}$ may be related to the eigenvalues $\{\epsilon_a, \epsilon_b, \epsilon_c\}$ of $\underline{\underline{\epsilon}}_{CTF}$ via one of several homogenization formalisms, including the Maxwell Garnett formalism [22], the Bragg–Pippard formalism [1], and the Bruggeman formalism [2]. We implement here the last-named formalism which has been widely used in optics [29], because it treats the region occupied by the deposited material and the void region symmetrically, unlike the other two formalisms.

Let us introduce the dyadic

$$\underline{\underline{b}} = f \underline{\underline{a}}_s + (1 - f) \underline{\underline{a}}_f, \quad (6)$$

which is the volume-fraction-weighted sum of the two polarizability density dyadics [2, 30]

$$\begin{aligned} \underline{\underline{a}}_s &= \epsilon_0 \left[n_s^2 \underline{\underline{I}} - (\epsilon_a \underline{u}_z \underline{u}_z + \epsilon_b \underline{u}_x \underline{u}_x + \epsilon_c \underline{u}_y \underline{u}_y) \right] \\ &\quad \cdot \left\{ \underline{\underline{I}} + i\omega \epsilon_0 \underline{\underline{D}}_s \cdot \left[n_s^2 \underline{\underline{I}} - (\epsilon_a \underline{u}_z \underline{u}_z + \epsilon_b \underline{u}_x \underline{u}_x + \epsilon_c \underline{u}_y \underline{u}_y) \right] \right\}^{-1} \end{aligned} \quad (7)$$

and

$$\begin{aligned} \underline{\underline{a}}_f &= \epsilon_0 \left[\underline{\underline{I}} - (\epsilon_a \underline{u}_z \underline{u}_z + \epsilon_b \underline{u}_x \underline{u}_x + \epsilon_c \underline{u}_y \underline{u}_y) \right] \\ &\quad \cdot \left\{ \underline{\underline{I}} + i\omega \epsilon_0 \underline{\underline{D}}_f \cdot \left[\underline{\underline{I}} - (\epsilon_a \underline{u}_z \underline{u}_z + \epsilon_b \underline{u}_x \underline{u}_x + \epsilon_c \underline{u}_y \underline{u}_y) \right] \right\}^{-1}. \end{aligned} \quad (8)$$

Herein, the depolarization dyadics

$$\begin{aligned} \underline{\underline{D}}_s &= \frac{1}{i\omega \epsilon_0} \frac{2}{\pi} \int_{\phi=0}^{\pi/2} d\phi \int_{\theta=0}^{\pi/2} d\theta \\ &\quad \sin \theta \frac{\frac{\cos^2 \theta}{\gamma_\tau^2} \underline{u}_x \underline{u}_x + \sin^2 \theta \left(\cos^2 \phi \underline{u}_z \underline{u}_z + \frac{\sin^2 \phi}{\gamma_b^2} \underline{u}_y \underline{u}_y \right)}{\epsilon_b \frac{\cos^2 \theta}{\gamma_\tau^2} + \sin^2 \theta \left(\epsilon_a \cos^2 \phi + \epsilon_c \frac{\sin^2 \phi}{\gamma_b^2} \right)}, \end{aligned} \quad (9)$$

and

$$\begin{aligned} \underline{\underline{D}}_f &= \frac{1}{i\omega \epsilon_0} \frac{2}{\pi} \int_{\phi=0}^{\pi/2} d\phi \int_{\theta=0}^{\pi/2} d\theta \\ &\quad \sin \theta \frac{\cos^2 \theta \underline{u}_x \underline{u}_x + \sin^2 \theta \left(\cos^2 \phi \underline{u}_z \underline{u}_z + \sin^2 \phi \underline{u}_y \underline{u}_y \right)}{\epsilon_b \cos^2 \theta + \sin^2 \theta \left(\epsilon_a \cos^2 \phi + \epsilon_c \sin^2 \phi \right)} \end{aligned} \quad (10)$$

are straightforwardly evaluated by numerical means. According to the Bruggeman homogenization formalism, the three parameters $\{n_s, f, \gamma_b\}$ satisfy the three nonlinear equations

$$b_\ell(n_s, f, \gamma_b) = 0, \quad (\ell = x, y, z), \quad (11)$$

where b_ℓ are the three nonzero components of the diagonal dyadic $\underline{\underline{b}}$; i.e.,

$$\underline{\underline{b}} = b_x \underline{\underline{u}}_x \underline{\underline{u}}_x + b_y \underline{\underline{u}}_y \underline{\underline{u}}_y + b_z \underline{\underline{u}}_z \underline{\underline{u}}_z. \quad (12)$$

Usually, the process of homogenization is applied in a forward sense, to provide a nanoscopic-to-continuum model. Thereby, the relative permittivity parameters $\{\epsilon_a, \epsilon_b, \epsilon_c\}$ may be estimated from a knowledge of the nanoscale parameters $\{n_s, f, \gamma_b\}$. However, the nanoscale parameters of CTFs are generally unknown whereas $\{\epsilon_a, \epsilon_b, \epsilon_c\}$ may be measured. In order to estimate $\{n_s, f, \gamma_b\}$ from a knowledge of $\{\epsilon_a, \epsilon_b, \epsilon_c\}$, the inverse homogenization process is needed. Formal expressions of the inverse Bruggeman formalism are available [31], but in certain cases these formal expressions may be ill-defined [32]. In practice, it is more convenient to implement a direct numerical method to compute $\{n_s, f, \gamma_b\}$, as described in the next section.

4 Numerical implementation

Solutions to Eqs. (11) may be computed using a modified Newton–Raphson technique [33, 34]. In the recursive scheme implemented here, the estimated solutions at step $k + 1$, namely $\{n_s^{(k+1)}, f^{(k+1)}, \gamma_b^{(k+1)}\}$, are derived from those at step k , namely $\{n_s^{(k)}, f^{(k)}, \gamma_b^{(k)}\}$, via

$$\left. \begin{aligned} n_s^{(k+1)} &= n_s^{(k)} - \frac{b_x(n_s^{(k)}, f^{(k)}, \gamma_b^{(k)})}{\frac{\partial}{\partial n_s} b_x(n_s^{(k)}, f^{(k)}, \gamma_b^{(k)})} \\ f^{(k+1)} &= f^{(k)} - \frac{b_y(n_s^{(k+1)}, f^{(k)}, \gamma_b^{(k)})}{\frac{\partial}{\partial f} b_y(n_s^{(k+1)}, f^{(k)}, \gamma_b^{(k)})} \\ \gamma_b^{(k+1)} &= \gamma_b^{(k)} - \frac{b_z(n_s^{(k+1)}, f^{(k+1)}, \gamma_b^{(k)})}{\frac{\partial}{\partial \gamma_b} b_z(n_s^{(k+1)}, f^{(k+1)}, \gamma_b^{(k)})} \end{aligned} \right\}. \quad (13)$$

In order for the scheme (13) to converge, it is crucial that the initial estimate $\{n_s^{(0)}, f^{(0)}, \gamma_b^{(0)}\}$ be sufficiently close to the true solution. A suitable initial estimate may be found by exploiting the forward Bruggeman formalism, as follows.

Let $\tilde{\epsilon}_{a,b,c}$ denote estimates of the CTF permittivity parameters $\epsilon_{a,b,c}$, computed using the forward Bruggeman formalism for physically reasonable ranges of the parameters n_s , f and γ_b , namely $n_s \in (n_s^L, n_s^U)$, $f \in (f^L, f^U)$ and $\gamma_b \in (\gamma_b^L, \gamma_b^U)$. Then:

- (i) Fix $n_s = (n_s^L + n_s^U)/2$ and $\gamma_b = (\gamma_b^L + \gamma_b^U)/2$. For all values of $f \in (f^L, f^U)$, identify the value f^* for which the quantity

$$\Delta = \sqrt{(\epsilon_a - \tilde{\epsilon}_a)^2 + (\epsilon_b - \tilde{\epsilon}_b)^2 + (\epsilon_c - \tilde{\epsilon}_c)^2} \quad (14)$$

is minimized.

- (ii) Fix $f = f^*$ and $\gamma_b = (\gamma_b^L + \gamma_b^U)/2$. For all values of $n_s \in (n_s^L, n_s^U)$, identify the value n_s^* for which Δ is minimized.

- (iii) Fix $f = f^*$ and $n_s = n_s^*$. For all values of $\gamma_b \in (\gamma_b^L, \gamma_b^U)$, identify the value γ_b^* for which Δ is minimized.

The steps (i)–(iii) are repeated, using n_s^* and γ_b^* as the fixed values of n_s and γ_b in step (i), and γ_b^* as the fixed value of γ_b in step (ii), until Δ becomes sufficiently small. In our numerical experiments, we found that when $\Delta < 0.01$, the values of n_s^* , f^* and γ_b^* provide suitable initial estimates for the modified Newton–Raphson scheme (13).

5 Numerical results

We considered CTFs made from three different materials: the oxides of tantalum, titanium and zirconium. Experimental studies [26] have revealed that the permittivity parameters for these CTFs may be expressed as

$$\left. \begin{aligned} \epsilon_a &= (n_{a0} + n_{a1} v + n_{a2} v^2)^2 \\ \epsilon_b &= (n_{b0} + n_{b1} v + n_{b2} v^2)^2 \\ \epsilon_c &= (n_{c0} + n_{c1} v + n_{c2} v^2)^2 \\ v &= 2\chi_v/\pi \end{aligned} \right\}, \quad (15)$$

wherein the vapor incidence angle $\chi_v \in (0, \pi/2]$ is related to the column inclination angle by the coefficient \bar{m} , per

$$\tan \chi = \bar{m} \tan \chi_v. \quad (16)$$

Table 1 contains values of the ten coefficients n_{a0} to \bar{m} of CTFs of the three different materials. Although the bulk refractive indexes of all three oxides are quite close to each other, the coefficients n_{a0} to m of the three types of CTFs are quite different, as indeed are also their constitutive parameters $\epsilon_{a,b,c}$ [35]. These differences arise, in significant measure, due to the dependence of the growth dynamics of a CTF on the evaporated bulk material [36, 37].

Table 1: Coefficients appearing in Eqs. (15), obtained from the experimental findings of Hodgkinson *et al.* [26] on CTFs, when the free-space wavelength is 633 nm.

material	n_{a0}	n_{a1}	n_{a2}	n_{b0}	n_{b1}	n_{b2}
tantalum oxide	1.1961	1.5439	-0.7719	1.4600	1.0400	-0.5200
titanium oxide	1.0443	2.7394	-1.3697	1.6765	1.5649	-0.7825
zirconium oxide	1.2394	1.2912	-0.6456	1.4676	0.9428	-0.4714

material	n_{c0}	n_{c1}	n_{c2}	\bar{m}
tantalum oxide	1.3532	1.2296	-0.6148	3.1056
titanium oxide	1.3586	2.1109	-1.0554	2.8818
zirconium oxide	1.3861	0.9979	-0.4990	3.5587

The nanoscale parameters $\{n_s, f, \gamma_b\}$ were estimated for the three CTFs using the modified Newton–Raphson technique (13), with initial guesses $\{n_s^{(0)}, f^{(0)}, \gamma_b^{(0)}\}$ deduced by scanning the solution space of $\{\tilde{\epsilon}_a, \tilde{\epsilon}_b, \tilde{\epsilon}_c\}$ with $n_s^L = 1$, $n_s^U = 4$, $f^L = 0.2$, $f^U = 0.9$, $\gamma_b^L = 0.5$ and $\gamma_b^U = 3$.

The computed nanoscale parameters n_s , f , and γ_b , respectively, are plotted in Figs. 1–3, against $\chi_v \in (12^\circ, 90^\circ)$ for the CTFs fabricated by evaporating any one of the three bulk materials. The plots in Fig. 1 show that n_s for CTFs made by evaporating any of the three bulk materials to be largely insensitive to χ_v . In contrast, the volume fractions f displayed in Fig. 2 for all three materials increase rapidly as χ_v increases, in general accord with the observation that mass density of a CTF varies as $(1 + \sin \chi_v)^{-1} \sin \chi_v$ [38]. The

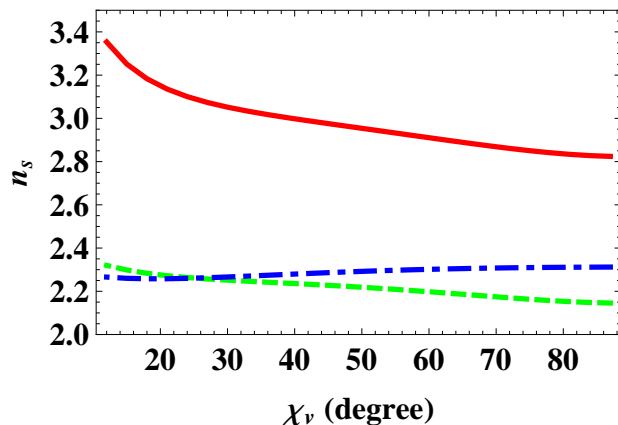


Figure 1: The quantity n_s plotted against χ_v (in degree) for CTFs made from evaporating titanium oxide (red, solid curve), tantalum oxide (green, dashed curve) and zirconium oxide (blue, broken dashed curve), as computed using the inverse Bruggeman formalism.

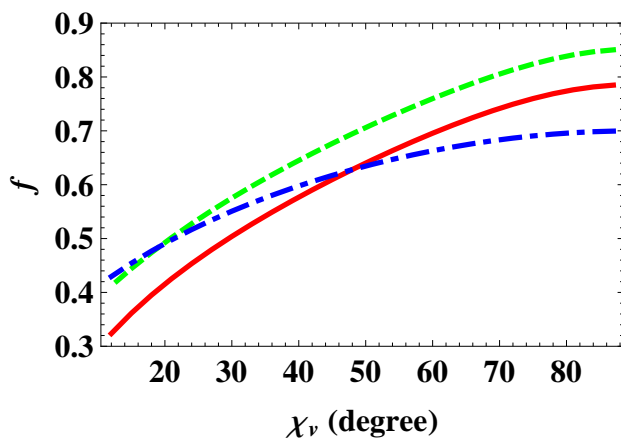


Figure 2: As Fig. 1 except that the quantity plotted against χ_v is f .

shape parameters γ_b displayed in Fig. 3 for CTFs of all three evaporated bulk materials decrease rapidly towards unity as χ_v increases. This is in accord with the observation that CTFs deposited with $\chi_v = 90^\circ$ are macroscopically uniaxial rather than biaxial [1].

6 Concluding remarks

In order to exploit the considerable potential that CTFs possess for widespread applications such as optical sensors of analytes, it is vital that they be reliably characterized at the nanoscale. Our theoretical and numerical study has demonstrated that the inverse Bruggeman homogenization formalism provides a practicable means for this characterization, in terms of three nanoscale parameters. Thus, a key step towards the intelligent design and development of CTF-based (and other STF-based [39]) optical sensors has been taken.

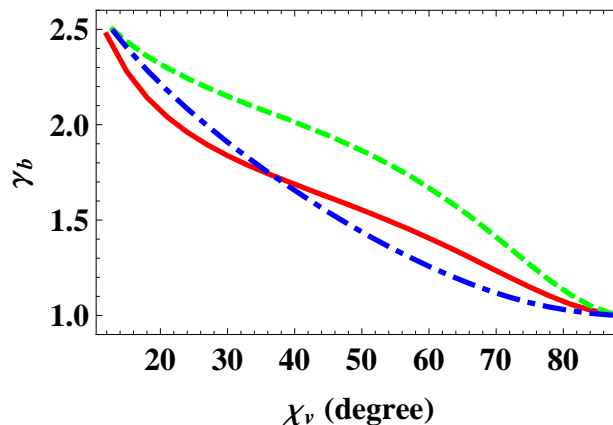


Figure 3: As Fig. 1 except that the quantity plotted against χ_v is γ_b .

Acknowledgments: TGM is supported by a Royal Academy of Engineering/Leverhulme Trust Senior Research Fellowship. AL thanks the Binder Endowment at Penn State for partial financial support of his research activities.

References

- [1] I. J. Hodgkinson, Q. H. Wu, *Birefringent Thin Films and Polarizing Elements*, World Scientific, Singapore (1998).
- [2] A. Lakhtakia, R. Messier, *Sculptured Thin Films: Nanoengineered Morphology and Optics*, SPIE Press, Bellingham, WA, USA (2005).
- [3] A. Lakhtakia, R. Messier, M. J. Brett, and K. Robbie, “Sculptured thin films (STFs) for optical, chemical and biological applications,” *Innovat. Mater. Res.* **1**, 165–176 (1996).
- [4] A. Lakhtakia, “On bioluminescent emission from chiral sculptured thin films,” *Opt. Commun.* **188**, 313–320 (2001) [doi:10.1016/S0030-4018(00)01144-5].
- [5] A. Lakhtakia, M. W. McCall, J. A. Sherwin, Q. H. Wu, and I. J. Hodgkinson, “Sculptured–thin–film spectral holes for optical sensing of fluids,” *Opt. Commun.* **194**, 33–46 (2001) [doi:10.1016/S0030-4018(01)01225-1].
- [6] J. J. Steele, A. C. van Popta, M. M. Hawkeye, J. C. Sit, and M. J. Brett, “Nanostructured gradient index optical filter for high–speed humidity sensing,” *Sens. Actuat. B: Chem.* **120**, 213–219 (2006) [doi:10.1016/j.snb.2006.02.003].
- [7] S. M. Pursel and M. W. Horn, “Prospects for nanowire sculptured–thin–film devices,” *J. Vac. Sci. Technol. B* **25**, 2611–2615 (2007) [doi:10.1116/1.2787749].
- [8] A. Lakhtakia, “Toward optical sensing of metal nanoparticles using chiral sculptured thin films,” *J. Nanophoton.* **1**, 019502 (2007) [doi:10.1117/1.2753364].
- [9] T. G. Mackay and A. Lakhtakia, “Theory of light emission from a dipole source embedded in a chiral sculptured thin film,” *Opt. Express* **15** 14689–14703 (2007) [doi:10.1364/OE.15.014689]. Erratum **16**, 3659 (2008) [doi:10.1364/OE.16.003659].

- [10] M. A. Motyka and A. Lakhtakia, “Multiple trains of same-color surface plasmon-polaritons guided by the planar interface of a metal and a sculptured nematic thin film,” *J. Nanophoton.* **2**, 021910 (2008) [doi:10.1117/1.3033757].
- [11] J. A. Polo Jr. and A. Lakhtakia, “On the surface plasmon polariton wave at the planar interface of a metal and a chiral sculptured thin film,” *Proc. R. Soc. Lond. A* **465**, 87–107 (2009) [doi:10.1098/rspa.2008.0211].
- [12] R. Messier, T. Takamori, and R. Roy, “Structure-composition variation in rf-sputtered films of Ge caused by process parameter changes,” *J. Vac. Sci. Technol.* **13**, 1060–1065 (1976) [doi:10.1116/1.569060].
- [13] J. R. Blanco, P. J. McMarr, J. E. Yehoda, K. Vedam, and R. Messier, “Density of amorphous germanium films by spectroscopic ellipsometry,” *J. Vac. Sci. Technol. A* **4** 577–582 (1986) [doi:10.1116/1.573851].
- [14] F. Walbel, E. Ritter, and R. Linsbod, “Properties of TiO_x films prepared by electron-beam evaporation of titanium and titanium suboxides,” *Appl. Opt.* **42** 4590–4593 (2003) [doi:10.1364/AO.42.004590].
- [15] H. A. Macleod, *Thin-Film Optical Filters, 3rd ed.*, Institute of Physics, Bristol, UK (2001).
- [16] S. Brunauer, P. H. Emmett, and E. Teller, “Adsorption of gases in multimolecular layers,” *J. Am. Chem. Soc.* **60**, 309–319 (1938) [doi:10.1021/ja01269a023].
- [17] G. Bomchil, R. Herino, K. Barla, and J. C. Pfister, “Pore size distribution in porous silicon studied by adsorption isotherms,” *J. Electrochem. Soc.* **130**, 1611–1614 (1983) [doi:10.1149/1.2120044].
- [18] J. V. Ryan, M. Horn, A. Lakhtakia, and C. G. Pantano, “Characterization of sculptured thin films,” *Proc. SPIE* **5593**, 643–649 (2004) [doi:10.1117/12.573910].
- [19] G. B. Smith, “Effective medium theory and angular dispersion of optical constants in films with oblique columnar structure,” *Opt. Commun.* **71**, 279–284 (1989) [doi:10.1016/0030-4018(89)90008-4].
- [20] H. Wang, “Assessment of optical constants of multilayer thin films with columnar-structure-induced anisotropy,” *J. Phys. D: Appl. Phys.* **28**, 571–575 (1995) [doi:10.1088/0022-3727/28/3/019].
- [21] A. Lakhtakia and W. S. Weiglhofer, “Significance of cross-sectional morphology for Motohiro-Taga interfaces,” *Optik* **110**, 33–36 (1999).
- [22] L. Ward, *The Optical Constants of Bulk Materials and Films, 2nd ed.*, Institute of Physics, Bristol, UK (2000).
- [23] T. G. Mackay, “Lewin’s homogenization formula revisited for nanocomposite materials,” *J. Nanophoton.* **2**, 029503 (2008) [doi:10.1117/1.3028260].
- [24] J. A. Sherwin, A. Lakhtakia, and I. J. Hodgkinson, “On calibration of a nominal structure-property relationship model for chiral sculptured thin films by axial transmittance measurements,” *Opt. Commun.* **209**, 369–375 (2002) [doi:10.1016/S0030-4018(02)01672-3].
- [25] A. Shalabney, A. Lakhtakia, I. Abdulhalim, A. Lahav, C. Patzig, I. Hazeq, A. Karabchevsky, B. Rauschenbach, F. Zhang, and J. Xu, *Photon. Nanostruct.* [doi:10.1016/j.photonics.2009.03.003].
- [26] I. Hodgkinson, Q. h. Wu, and J. Hazel, “Empirical equations for the principal refractive indices and column angle of obliquely deposited films of tantalum oxide, titanium oxide, and zirconium oxide,” *Appl. Opt.* **37**, 2653–2659 (1998) [doi:10.1364/AO.37.002653].
- [27] N. A. Beaudry, Y. Zhao, and R. Chipman, “Dielectric tensor measurement from a single Mueller matrix image,” *J. Opt. Soc. Am. A* **24**, 814–824 (2007) [doi:10.1364/JOSAA.24.000814].

- [28] W. S. Weiglhofer, A. Lakhtakia, and B. Michel, “Maxwell Garnett and Bruggeman formalisms for a particulate composite with bianisotropic host medium,” *Microwave Opt. Technol. Lett.* **15**, 263–266 (1997) [doi:10.1002/(SICI)1098-2760(199707)15:4<263::AID-MOP19>3.0.CO;2-8]. Erratum **22**, 221 (1999) [doi:10.1002/(SICI)1098-2760(19990805)22:3<221::AID-MOP21>3.0.CO;2-R].
- [29] A. Lakhtakia, Ed., *Selected Papers on Linear Optical Composite Materials*, SPIE Optical Engineering Press, Bellingham, WA, USA (1996).
- [30] B. Michel, “Recent developments in the homogenization of linear bianisotropic composite materials,” in *Electromagnetic Fields in Unconventional Materials and Structures*, O. N. Singh and A. Lakhtakia, Eds., pp.39–82, Wiley, New York, NY, USA (2000).
- [31] W. S. Weiglhofer, “On the inverse homogenization problem of linear composite materials,” *Microwave Opt. Technol. Lett.* **28**, 421–423 (2001) [doi:10.1002/1098-2760(20010320)28:6<421::AID-MOP1059>3.0.CO;2-1].
- [32] E. Cherkaev, “Inverse homogenization for evaluation of effective properties of a mixture,” *Inverse Problems* **17**, 1203–1218 (2001) [doi:10.1088/0266-5611/17/4/341].
- [33] P. A. Stark, *Introduction to Numerical Methods*, Macmillan, New York, NY, USA (1970).
- [34] R. D. Kampia and A. Lakhtakia, “Bruggeman model for chiral particulate composites,” *J. Phys. D: Appl. Phys.* **25**, 1390–1394 (1992) [doi:10.1088/0022-3727/25/10/002].
- [35] F. Chiadini and A. Lakhtakia, “Gaussian model for refractive indexes of columnar thin films and Bragg multilayers,” *Opt. Commun.* **231**, 257–261 (2004) [doi:10.1016/j.optcom.2003.12.030]. Erratum **265**, 366 (2006) [doi:10.1016/j.optcom.2006.06.030].
- [36] R. Messier, V. C. Venugopal, and P. D. Sunal, “Origin and evolution of sculptured thin films,” *J. Vac. Sci. Technol. A* **18**, 1538–1545 (2000) [doi:10.1116/1.582381].
- [37] R. Messier, “The nano–world of thin films,” *J. Nanophoton.* **2**, 021995 (2008) [doi:10.1117/1.3000671].
- [38] R. N. Tait, T. Smy, and M. J. Brett, “Modelling and characterization of columnar growth in evaporated films,” *Thin Solid Films* **226**, 196–201 (1993) [doi:10.1016/0040-6090(93)90378-3].
- [39] I. Abdulhalim, M. Zourob, and A. Lakhtakia, “Overview of optical biosensing techniques,” in *Handbook of Biosensors and Biochips*, R. S. Marks, D. C. Cullen, I. Karube, C. R. Lowe, and H. H. Weetall, Eds., pp.413–446, Wiley, Chicester, UK (2007).